
Since January 2020 Elsevier has created a COVID-19 resource centre with free information in English and Mandarin on the novel coronavirus COVID-19. The COVID-19 resource centre is hosted on Elsevier Connect, the company's public news and information website.

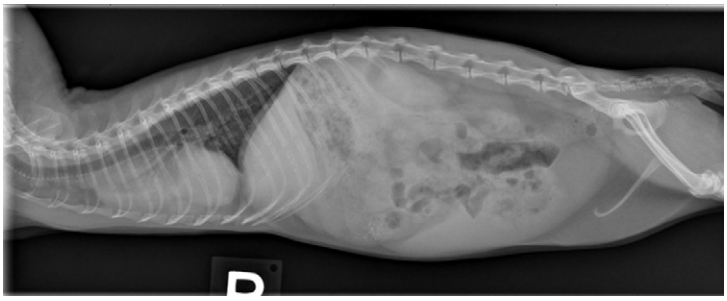

**FIGURE 1.** Right lateral whole-body radiograph.

An 18-month-old, 1.24-kg male castrated ferret was presented to the University of Illinois Veterinary Teaching Hospital (Urbana, IL USA) for a 4-week history of lethargy, inappetance, possible straining to urinate/defecate, and swelling with erythema of the gingiva adjacent to the left maxillary canine. A leukocytosis and hyperglobulinemia were also noted by the referring veterinarian 1 week before presentation.

The patient was quiet, inquisitive, and alert on initial presentation, but became notably depressed soon thereafter. Body condition score was an estimated 3 out of 5. The patient was painful on manipulation of the mouth, likely because of the gingival swelling and erythema. Thoracic auscultation revealed a sinus arrhythmia and mild end-inspiratory wheeze with possible mild expiratory effort. Temperature, heart rate, and respiratory rate were 98.6°F, 250 beats/min, and 42 breaths/min, respectively. Abdominal palpation revealed an enlarged spleen and pain on caudal abdominal manipulation. No other abnormalities were detected on physical examination. Based on the history and physical examination findings, the ferret was admitted for additional diagnostic testing and therapy.

The ferret was anesthetized via facemask with 5% isoflurane (IsoFlo; Abbott Laboratories, North Chicago, IL USA) and oxygen (1 L/min). Once the animal was induced, it was maintained at 1.5% isoflurane and 1 L/min oxygen. A blood sample (2 mL) was collected from the cranial vena cavae and submitted for a complete blood count (CBC) and plasma biochemistry testing. Whole-body survey radiographs (Eklin EDR6 Clinical Digital Radiography System; Eklin Medical Systems, Inc., Santa Clara, CA USA) (Figs. 1 and 2) were also taken while the animal was anesthetized.

The CBC and plasma biochemistry analysis revealed the following abnormalities: normocytic normochromic anemia (hematocrit 24.9%; reference: 36-48); mild leukocytosis (white blood cell count 10.1 $\times$ $10^3/\mu$L; reference: 4.3-10.7) with a left shift (6% bands; reference: 0%); mild elevation in blood urea nitrogen (37 mg/dL; reference: 18-32); mild hypoalbuminemia (2 g/dL; reference: 2.5-4.0); and persistent hyperglobulinemia (7.1 g/dL; reference: 2.0-4.2).[1]

*At this time, evaluate the history, physical examination findings, CBC and plasma biochemistry results, and Figures 1 and 2. Formulate a list of differential diagnoses, additional diagnostic tests, and treatment plan before proceeding.*

**FIGURE 2.** Ventrodorsal whole-body radiograph.

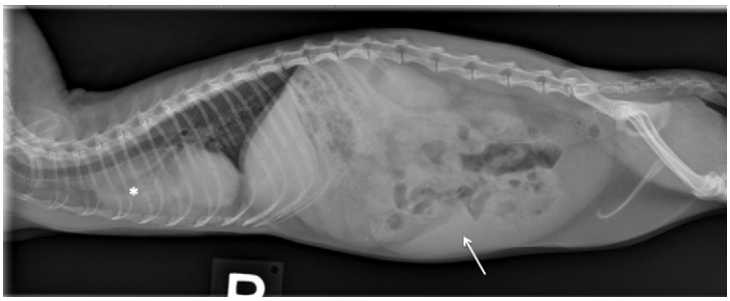

**FIGURE 3.** Right lateral whole-body radiograph. Note the soft tissue opaque mass (*) in the cranioventral thorax resulting in dorsal tracheal displacement and caudodorsal displacement of the cardiac silhouette. An enlarged, rounded splenic tail can be seen lining the caudoventral abdominal cavity (arrow).

## DIAGNOSIS

Initial diagnostic imaging of the ferret included whole-body right lateral and ventrodorsal view radiographs. Radiographs revealed widening of the cranial mediastinum due to a soft tissue opaque mass resulting in dorsal tracheal deviation (Figs. 3 and 4). Left cranial lung field alveolar pulmonary changes were also noted resulting in border effacement with the adjacent margin of the cardiac silhouette. The spleen showed evidence of marked enlargement with rounded peripheral margins (Fig. 3). Hepatic margins were also rounded in appearance. Given the noted hepatosplenomegaly in the face of a concurrent cranial mediastinal mass, lymphoma was considered the most likely differential with cranial mediastinal lymph node or thymic involvement; thymoma was considered an alternative differential diagnosis. Left cranial lung field changes were considered to be most likely secondary due to atelectasis given sedation at the time of image acquisition.

**FIGURE 4.** Ventrodorsal whole-body radiograph. Note the soft tissue opaque mass effect occupying the width of the cranial thoracic cavity along midline (between arrows).

Radiographic assessment was immediately followed by combined abdominal and limited thoracic ultrasound. A microconvex curvilinear array transducer (3-9 MHz) and linear array transducer (4-13 MHz) were used for routine B-mode imaging (MyLab70 XVG; Esaote, Indianapolis, IN USA). Abdominal ultrasound revealed hepatosplenomegaly consistent with the radiographic findings. Jejunal lymphadenopathy was also noted in addition to a small volume of peritoneal free fluid. Limited thoracic ultrasound revealed both sternal lymphadenopathy and a large hypoechoic cranial mediastinal mass; the caudal limit of which was intimately associated with the cranial margin of the cardiac silhouette. Upon color Doppler interrogation, this mass was considered to be moderately vascularized. Ultrasound-guided fine-needle aspiration of the cranial mediastinal mass and an enlarged jejunal lymph node were performed; the former revealed cells consistent with lymphoid tissue and the latter was cytologically inconclusive.

After the ultrasound examination, initial supportive care was instituted, including furosemide

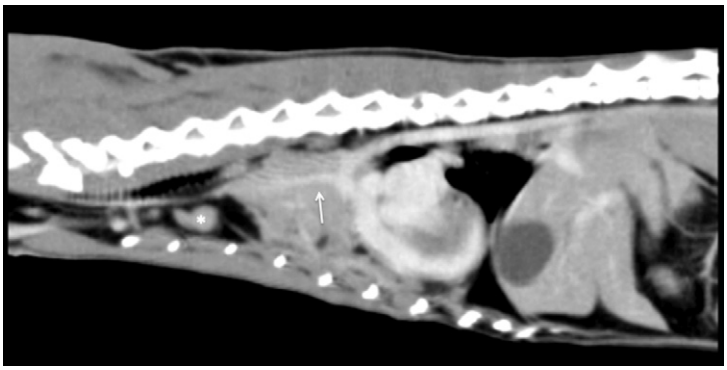

**FIGURE 5.** Sagittal plane CT reconstruction of the thorax displayed in a soft tissue window post-administration of contrast medium. Note the intimate association of the cranial mediastinal mass lesion with the major thoracic vasculature (arrow). An enlarged, rounded sternal lymph node can be seen dorsal to the level of the second sternebra (*).

(2 mg/kg intramuscularly every 12 hours, Salix; Intervet, Inc., Millsboro, DE USA), enrofloxacin (5 mg/kg orally every 12 hours, Baytril; Bayer, Shawnee Mission, KS USA), meloxicam (0.3 mg/kg orally every 24 hours, Boehringer Ingelheim, St. Joseph, MO USA), Carnivore Care (45 mL orally every 24 hours, Oxbow, Inc., Murdock, NE USA), Lactated Ringer's solution (24 mL subcutaneously every 8 hours, Abbott Laboratories), and butorphanol (0.08 mg/kg subcutaneously every 12 hours, Torbugesic; Ft. Dodge Animal Health, Ft. Dodge, IA USA).

Given the high suspicion for neoplasia in the absence of a definitive diagnosis, thoracic computed tomography (CT) was pursued the following day in an attempt to better characterize the origin/extent of the cranial mediastinal mass using a 16-slice helical CT scanner (LightSpeed; GE Healthcare, Milwaukee, WI USA). The ferret was anesthetized as previously described for the procedure. Primary transverse CT acquisition parameters included a 2.5-mm-slice thickness with 1.25-mm overlap, pitch of 0.938:1, 0.8-second rotation time, 100 kV, and 100 mA. Subsequent multiplanar reformatting was performed to obtain images with a 0.625-mm-slice thickness. After survey thoracic CT, 2-mL/kg (600-mg/kg) nonionic iodinated contrast medium (Omnipaque 300 iohexol injection; GE Healthcare, Princeton, NJ USA) was administered intraosseously as a bolus and postcontrast images were obtained. CT evaluation revealed a large, cystic heterogeneously contrast-enhancing, soft tissue–attenuating cranial mediastinal mass extending from the thoracic inlet to the cranial aspect of the heart and from the left to right thoracic wall. This mass completely encircled the brachycephalic trunk and partially encircled the cranial vena cava. The mass measured an estimated 18 mm in height × 27 mm in width × 31 mm in length. Complete alveolarization of the left and right cranial lung lobes with partial alveolar disease in the right middle lung lobe was also noted. A mild amount of pleural-free fluid was identified in addition to sternal lymphadenopathy. Thymoma and thymic lymphoma remained the most likely differentials for the cranial mediastinal mass. Sternal lymphadenopathy was considered either metastatic or alternatively a normal variant. Pulmonary changes were still considered to be most likely secondary to atelectasis with possible concurrent edema.

A sagittal plane reconstruction is provided and shown in a venous phase (Fig. 5), highlighting the size and extent of the mass including the intimate integration of the mass with the major cranial thoracic vasculature and cranial margin of the cardiac silhouette. Sternal lymph node enlargement is also clearly seen in Figure 5. Postcontrast reformatted images are also displayed in a 3D-volume–rendered image displayed with visible voxel values ranging from 107 to 549 (Fig. 6). The vascularized portion of the mass can be seen immediately cranial to the cardiac silhouette.

Percutaneous ultrasound-guided core biopsy (18 g) of the cranial mediastinal mass was attempted with the patient under isoflurane anesthesia after CT evaluation. After acquisition of 2 biopsy samples, the patient rapidly decompensated and went into respiratory and cardiac arrest. Cardiopulmonary resuscitation was attempted; however, it was ultimately unsuccessful.

Necropsy and histopathology were ultimately pursued, revealing severe, multisystemic, granulomatous mediastinitis, pneumonia, myocarditis (right auricle), hepatitis and lymphadenitis (sublumbar and mesenteric lymph nodes) consisting of densely cellular, coalescing aggregates of epithelioid and foamy macrophages with interspersed lymphocytes, plasma cells and neutrophils (Fig. 7). Presence of intralesional ferret coronavirus was confirmed by immunohistochemistry (Fig. 8) with an antibody specific for ferret coronavirus (Custom Monoclonals International; West Sacramento, CA USA). There was also evidence of pulmonary atelectasis secondary to hemothorax.

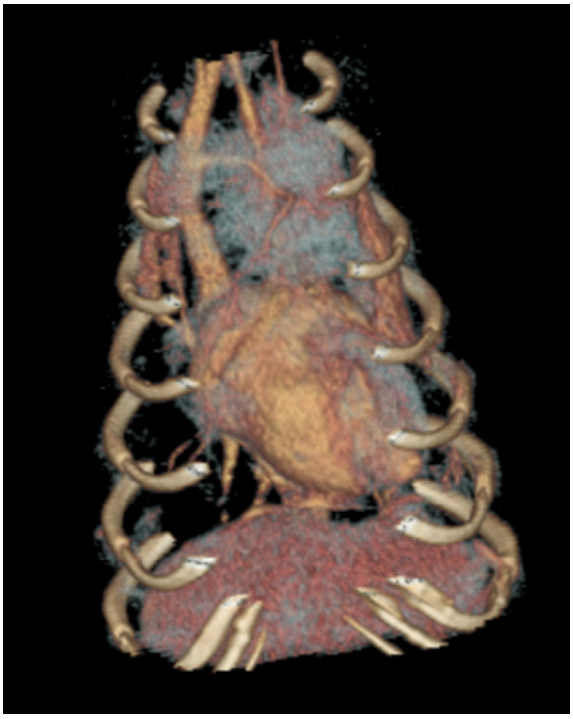

**FIGURE 6.** Dorsal plane 3D-volume–rendering CT obtained in the same postcontrast phase as in Figure 5. The sternebrae have been cropped to permit visualization of the ventral surface of the cardiac silhouette and cranial mediastinal mass. The cranial mediastinal mass is displayed in a bluish hue; note the marked tortuous vasculature embedded within the mass and intimate association of the mass with the adjacent cardiac silhouette and thoracic aorta.

## DISCUSSION

Cranial mediastinal mass lesions in the domestic ferret have been previously reported, most commonly in the context of lymphoma or thymic lymphoma.[2-5] Thymoma has also been reported in the adult ferret.[6] Given the possibility of multicentric disease, especially in the case of lymphoma, concurrent hepatosplenomegaly is not an unexpected finding, which was the case in the ferret described in this article. For this reason, multicentric lymphoma was considered the top differential diagnosis.

Infectious pyogranulomatous mediastinitis was recently reported for the first time in a case series including 3 domestic ferrets with *Pseudomonas luteola* infection. The clinical presentation was similar to that seen in this case with reported respiratory distress (all 3 cases) and evidence of hyperglobulinemia (1 case).[7] In a separate case series, cryptococcosis was reported as a possible infectious cause of mediastinal lymphadenopathy.[8] The case presented in this article is the first report of infectious pyogranulomatous mediastinitis being associated with ferret coronavirus.

The veterinary literature is extremely limited with respect to coronavirus infection in the domestic ferret. One of the earliest reports of coronavirus infection in ferrets described coronavirus-associated epizootic catarrhal enteritis. In that retrospective study, domestic ferrets with a clinical history of diarrhea and a lack of a definitive etiology, in addition to one or more of the following microscopic lesions: vacuolar degeneration and necrosis of villus enterocytes; villous atrophy, fusion, and blunting; and lymphoplasmacytic enteritis characterized by a subjective increase in number of intraepithelial lymphocytes, were evaluated. A total of 119 cases met the inclusion criteria that determined a definitive diagnosis. Coronavirus particles were identified in feces and jejunal enterocytes by use of transmission electron microscopy. Immunohistochemical staining of jejunal sections also revealed coronavirus antigens that were not detected in healthy ferrets or in ferrets with other gastrointestinal diseases.[9] In a later study using consensus polymerase chain reaction assays for the genus *Coronavirus*, followed by genomic sequencing and phylogenetic analyses, a separate group provided the first molecular evidence that the virus associated with epizootic catarrhal enteritis in ferrets was, in fact, a new coronavirus tentatively designated as "ferret enteric coronavirus."[10]

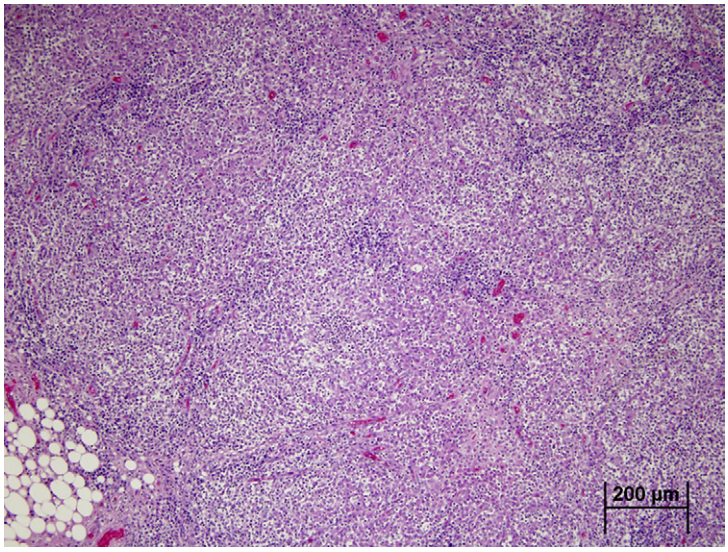


**FIGURE 7.** Histologic section of cranial mediastinum from a ferret with multisystemic coronavirus infection (ferret FIP). Cranial mediastinum is infiltrated by densely cellular, coalescing aggregates of epithelioid and foamy macrophages with interspersed lymphocytes, plasma cells, and neutrophils (granulomatous mediastinitis). Hematoxylin and eosin stain.

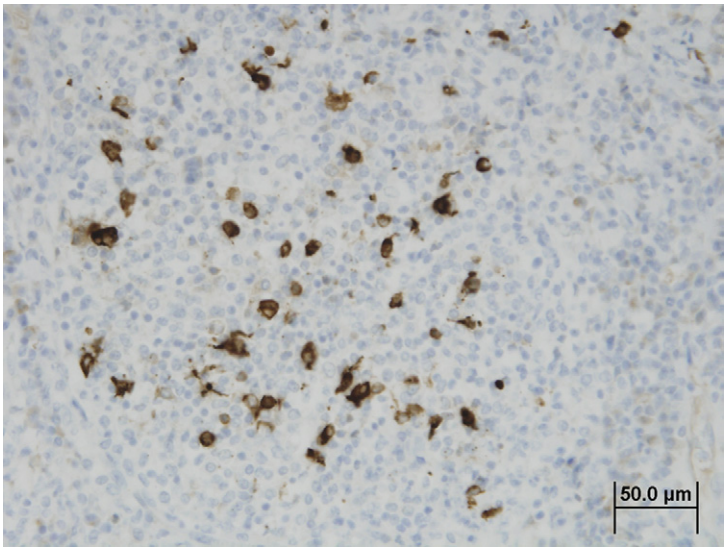


**FIGURE 8.** Histologic section of cranial mediastinum from a ferret with multisystemic coronavirus infection (ferret FIP). Intralesional coronavirus are positively labeled by immunohistochemistry with an antibody specific for ferret coronavirus (Custom Monoclonals International). Avidin-biotin complex method, hematoxylin counterstain.

Although uncomplicated epizootic catarrhal enteritis is considered to be self-limiting or treatable with supportive care and characterized by having high morbidity and low mortality rates, the multisystemic granulomatous coronavirus-associated disease identified in our case is characterized by a much more severe phenotype resembling feline infectious peritonitis (FIP), which is similarly caused by a feline coronavirus.

In cats, FIP is characterized by a fibrinous to granulomatous serositis with protein-rich effusions and multisystemic granulomatous inflammatory lesions. FIP-like antigen in ferrets has been described postmortem with lymph nodes and mesentery showing the greatest frequency and severity of multifocal granulomatous lesions, the majority of cases of which demonstrated immunohistological evidence of feline coronavirus.[11] Clinicopathologic features of a systemic coronavirus-associated disease resembling FIP in the domestic ferret were described shortly thereafter. Twenty-three ferrets diagnosed with systemic pyogranulomatous inflammation resembling FIP were enrolled in a case series. The average age at the time of diagnosis was 11 months, with progressive disease identified in all cases. Nonspecific clinical signs including anorexia, weight loss, diarrhea, and large palpable intraabdominal masses were common clinical findings, whereas neurological deficits, vomiting, and dyspnea were reported with less frequency. Hyperglobulinemia was documented in 9 ferrets, mild nonregenerative anemia in 11 ferrets, and thrombocytopenia in 3 ferrets. Mesenteric adipose tissue and lymph nodes, liver, kidney, spleen, and lung were all reported sites of grossly visible pyogranulomatous lesions. Immunohistochemically, all cases were positive for coronavirus antigen.[12] There were no reports of mediastinal or cardiac involvement. Diffuse granulomatous inflammation on serosal surfaces was identified in the heart of a single case in a separate study.[13]

In an attempt to improve antemortem diagnosis of systemic coronavirus infection in the domestic ferret, the radiographic and ultrasonographic findings in affected patients were later described. In all patients undergoing abdominal radiography, moderate to severe loss of the lumbar musculature was noted. Decreased peritoneal and retroperitoneal serosal detail, gas distension of the gastrointestinal tract, mid-abdominal soft tissue opaque masses, renomegaly, and splenomegaly were also reported to a variable degree. Ultrasonographic findings included peritoneal effusion, hyperechoic mesentery, mesenteric lymphadenopathy, ill-defined mixed echoic mass lesions, renomegaly, and pyelectasia. The authors concluded that imaging signs of peritonitis, mesenteric lymphadenopathy, and soft tissue abdominal masses are highly suspicious for systemic coronavirus infection. Hepatic and splenic changes were reportedly inconclusive.[14] This case report describes the first case of systemic coronavirus infection in a ferret with the development of a space-occupying cranial mediastinal mass; highlighting the importance of thoracic imaging in patients presenting with nonspecific clinical signs and laboratory changes that are suggestive of chronic inflammatory disease. Although lymphoma and thymoma remain the most commonly reported etiologies for development of cranial mediastinal mass lesions in young ferrets, infectious diseases, including coronavirus, should be considered; especially in the face of inconclusive cytological results. This is also the first report of contrast-enhanced thoracic CT characterization of a cranial mediastinal mass in the domestic ferret. Advanced imaging proved to be beneficial in more accurately characterizing the origin and vascularity of the primary mass lesion and permitted for more sensitive assessment of concurrent pulmonary lesions.

Currently there is no reported cure for ferrets afflicted with systemic coronavirus infection; most patients reportedly die or are humanely euthanized because of advanced multisystemic disease. However, survival of several months' duration up to more than 3 years (in a single case) has been described, so attempted therapy may

prove beneficial. Reported therapeutic strategies, most commonly those used in cats, include immunosuppressive therapy (prednisolone most commonly), immunomodulatory therapy, vasculitis therapy, and treatment of clinical disease (e.g., anti-emetics, gastro-protectants, antibiotic therapy, and nutritional support).[15]

This case was submitted by **Miriam M. Shanaman, VMD, Mark A. Mitchell, DVM, MS, PhD, Dip. ECZM (Herpetology), Samantha Haskins, DVM, Ken Welle, DVM, Dip. ABVP (Avian), Zoltan Demeter, DVM, PhD, Shih-Hsuan Hsiao, DVM, PhD, Sandra Murrell-Ritter, DVM, and Robert T. O'Brien, DVM, MS, Dip. ACVR,** from the University of Illinois, College of Veterinary Medicine, Urbana, IL 61802 USA, and All Creatures Animal Hospital, Urbana, IL 61801.


*1557-5063/12/2103-$30.00*
*http://dx.doi.org/10.1053/j.jepm.2012.06.001*

## REFERENCES

1. Quesenberry KE, Orcutt C: Basic approaches to veterinary care, in Quesenberry KE and Carpenter JW (eds): Ferrets, Rabbits and Rodents: Clinical Medicine and Surgery. St. Louis, MO, Elsevier, pp 13-26, 2012
2. Batchelder MA, Erdman SE, Li X, et al: A cluster of cases of juvenile mediastinal lymphoma in a ferret colony. Lab Anim Sci 46:271-274, 1996
3. Erdman SE, Brown SA, Kawasaki TA, et al: Clinical and pathologic findings in ferrets with lymphoma: 60 cases (1982-1994). J Am Vet Med Assoc 208:1285-1289, 1996
4. Coleman LA, Erdman SE, Schrenzel MD, et al: Immunophenotypic characterization of lymphomas from the mediastinum of young ferrets. Am J Vet Res 59:1281-1286, 1998
5. Onuma M, Kondo H, Ono S, et al: Cytomorphological and immunohistochemical features of lymphoma in ferrets. J Vet Med Sci 70:893-898, 2008
6. Taylor TG, Carpenter JL: Thymoma in two ferrets. Lab Anim Sci 45:363-365, 1995
7. Martínez J, Martorell J, Abarca ML, et al: Pyogranulomatous pleuropneumonia and mediastinitis in ferrets (*Mustela putorius furo*) associated with *Pseudomonas luteola* infection. J Comp Pathol 146:4-10, 2012
8. Malik R, Alderton B, Finlaison D, et al: Cryptococcosis in ferrets: a diverse spectrum of clinical disease. Aust Vet J 80:749-755, 2002
9. Williams BH, Kiupel M, West KH, et al: Coronavirus-associated epizootic catarrhal enteritis in ferrets. J Am Vet Med Assoc 217:526-530, 2000
10. Wise AG, Kiupel M, Maes RK: Molecular characterization of a novel coronavirus associated with epizootic catarrhal enteritis (ECE) in ferrets. Virolology 349:164-174, 2006
11. Martínez J, Ramis AJ, Reinacher M, et al: Detection of feline infectious peritonitis virus-like antigen in ferrets. Vet Rec 158:523, 2006
12. Garner MM, Ramsell K, Morera N, et al: Clinicopathologic features of a systemic coronavirus-associated disease resembling feline infectious peritonitis in the domestic ferret (*Mustela putorius*). Vet Pathol 45:236-246, 2008
13. Martínez J, Reinacher M, Perpiñán D, et al: Identification of Group 1 coronavirus antigen in multisystemic granulomatous lesions in ferrets. J Comp Path 138:54-58, 2008
14. Dominguez E, Novellas R, Moya A, et al: Abdominal radiographic and ultrasonographic findings in ferrets (*Mustela putorius furo*) with systemic coronavirus infection. Vet Rec 169:231, 2011
15. Murray J, Kiupel M, Maes RK: Ferret coronavirus-associated diseases. Vet Clin North Am Exot Anim Pract 13:543-560, 2010